

First-Principles Many-Body Investigation of Correlated Oxide Heterostructures: Few-Layer-Doped SmTiO_3

Frank Lechermann

¹ I. Institut für Theoretische Physik, Universität Hamburg,
D-20355 Hamburg, Germany
E-mail: Frank.Lechermann@physnet.uni-hamburg.de

² Institut für Keramische Hochleistungswerkstoffe, Technische Universität Hamburg-Harburg,
D-21073 Hamburg, Germany

Correlated oxide heterostructures pose a challenging problem in condensed matter research due to their structural complexity interweaved with demanding electron states beyond the effective single-particle picture. By exploring the correlated electronic structure of SmTiO_3 doped with few layers of SrO, we provide an insight into the complexity of such systems. Furthermore, it is shown how the advanced combination of band theory on the level of Kohn-Sham density functional theory with explicit many-body theory on the level of dynamical mean-field theory provides an adequate tool to cope with the problem. Coexistence of band-insulating, metallic and Mott-critical electronic regions is revealed in individual heterostructures with multi-orbital manifolds. Intriguing orbital polarizations, that qualitatively vary between the metallic and the Mott layers are also encountered.

1 Introduction

Research on oxide heterostructures emerged in the beginning of the 2000s as a novel topical field and belongs nowadays to a key focus in condensed matter and materials science (see e.g. Refs. 1–3 for reviews). Thanks to important advancements in experimental preparation techniques, the design of oxide materials, e.g. by joint layering of different bulk compounds, opens new possibilities to devise matter beyond nature’s original conception. Importantly, oxide heterostructures are not only relevant because of their potentially future technological importance, but they also challenge known paradigms in condensed matter physics. For instance, the obvious traditional separation of electronic materials into metals, band insulators or Mott insulators may be reconsidered in such materials. Since known bulk features of individual oxide building blocks disperse within a given heterostructure, characteristics of various electronic signatures may be detected^{4,5}. Notably, the distinguished role of interface physics within a demanding quantum-mechanical environment is one of main concerns in this area.

Density functional theory (DFT) in the Kohn-Sham representation is the standard tool for materials science starting from the atomic scale. However, this theoretical approach has its flaws for systems where the mutual interaction among the condensed matter electrons is comparable or even larger than the dispersion energy from hopping on the underlying lattice. For various reasons, many interesting oxide heterostructures are located in the latter regime, marking them as correlated oxide heterostructures (COHs). Modeling these fascinating designed materials, including the possibility for further engineering and prediction of intriguing phenomenology, therefore asks for a theoretical approach beyond effective single-particle theory. The combination of DFT with the explicit many-body framework of

dynamical mean-field theory (DMFT), the so-called DFT+DMFT method, represents such an approach (see e.g. Ref. 6 for a review).

In the present work, the charge self-consistent DFT+DMFT framework is put into practice to examine the correlated electronic structure of Mott-insulating SmTiO_3 doped with a few layers of SrO in a heterostructure architecture. This illustrates the challenges of COHs as well as the capabilities of advanced electronic structure theory to address those. Coexistence of different electronic phases is encountered, ranging from Mott-insulating, metallic up to band-insulating.

2 SrO doping layers in SmTiO_3

The rare-earth titanate SmTiO_3 is a distorted perovskite with orthorhombic $Pbnm$ crystal-symmetry group. Electronically, it is a Mott insulator in the bulk⁷, i.e. electrons are localized in real space and cannot metallize the compound via hopping because of the strong Coulomb repulsion. For this system, the most-relevant Coulomb impact is on the Ti- $3d$ shell, which is nominally filled with one electron since titanium is in a formal Ti^{3+} state. Moreover, calculations show that the electron dominantly resides in a single effective orbital of t_{2g} kind⁵, i.e. orbital polarization is an important issue.

In the present work, a well-defined doped Mott-insulator shall be investigated in a heterostructure architecture by inserting $n = 2, 4, 6$ layers of SrO into SmTiO_3 , thereby replacing SmO layers, respectively (see Fig. 1). Because of the different valence of Sr^{2+} compared to Sm^{3+} , this leads to an effective hole doping. Experimental transport studies of such systems have recently been performed^{8,9}. To model these complex COHs in a first-principles setting, superlattices based on 140-atom unit cells are here considered. They consist of 14 TiO_2 layers, and each layer is build from two symmetry-equivalent-treated Ti ions. With the inserted SrO layers, there are then 8 Ti sites different by symmetry, located in different layers (cf. Fig. 1). The original lattice parameters⁷ are brought in the directional form of the experimental works^{8,9}, but without lowering the $Pbnm$ symmetry. The original c -axis is *parallel* to the doping layer and the original a, b -axes are respectively inclined. With fixed lattice parameters, all atomic positions in the supercell are structurally relaxed

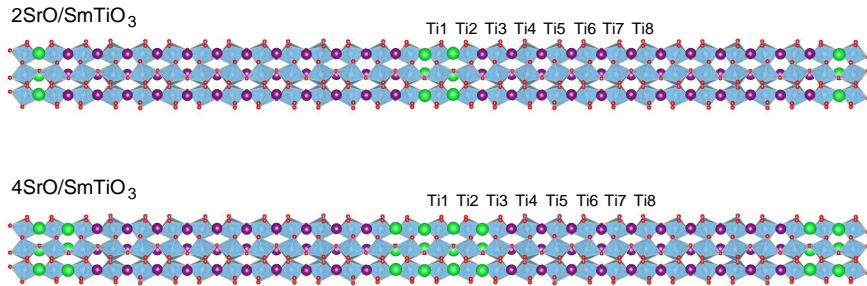


Figure 1. Supercells for the cases of 2- and 4SrO-layer doping of SmTiO_3 with the horizontal axis as the stacking direction (the $n = 6$ -layer system is constructed correspondingly). Sr: green, O: red, Sm: violet, Ti: blue. There are eight inequivalent Ti sites Ti1-8, describing the layer dependence of the electronic structure. Each layer consists of two Ti sites in the unit cell in order to incorporate the relevant orthorhombic distortions, but those intra-layer sites are treated equivalent by symmetry.

within DFT(GGA) until the maximum individual atomic force settles below 5 mRyd/a.u.. The lattice distortions introduced by the inserted SrO layers are well captured by this approach.

Note that the δ -doped case of $n = 1$ has been recently studied in detail by a similar approach⁵. In this respect, the present work advances on this previous study and renders it possible to follow the evolution of the correlated electronic structure of heterostructure-doped SmTiO₃ with further SrO layers.

3 Theoretical Approach

The charge self-consistent DFT+DMFT method combines band theory and many-body theory on an equal footing. The band-theoretical aspect is delivered on the DFT level, and through a downfolding to a correlated subspace of relevant sites and orbitals, electronic correlations are evaluated in the many-body scope. Those correlations define an electronic self-energy that reenters the DFT level in updating the Kohn-Sham potential. Thereby a self-consistency cycle is defined that at convergence provides the many-body electronic structure beyond conventional exchange-correlation functionals¹⁰⁻¹². For the DFT part, a mixed-basis pseudopotential coding¹³, based on norm-conserving pseudopotentials as well as a combined basis of localized functions and plane waves, is utilized. We here employ the generalized-gradient approximation (GGA) in the Perdew-Burke-Ernzerhof form¹⁴. Here, we aim for a description of SrO layers in SmTiO₃. The three Ti-3d(t_{2g}) orbitals, split-off from the remaining e_g orbitals of the full 3d shell, host the key-relevant single electron of SmTiO₃. The correlated subspace therefore consists of the effective Ti(t_{2g}) Wannier-like functions, i.e. is locally threefold. These functions are obtained from a projected-local-orbital formalism^{15,16}, using as projection functions the linear combinations of atomic t_{2g} orbitals. The latter diagonalize the Ti orbital-density matrix from DFT. A band manifold of 60 t_{2g} -dominated Kohn-Sham states at lower energy are used to realize the projection. Local Coulomb interactions within the correlated subspace in the so-called Slater-Kanamori form of a multi-orbital Hubbard Hamiltonian are parametrized by a Hubbard $U = 5$ eV and a Hund's coupling $J_H = 0.64$ eV¹⁷. The 8 coupled single-site DMFT impurity problems in the supercells are, respectively, solved by the continuous-time quantum Monte Carlo (QMC) scheme^{18,19} as implemented in the TRIQS package^{20,21}. A double-counting correction of fully-localized type²² is utilized, which accounts for correlation effects already included on the GGA level. About 40-50 DFT+DMFT iterations (of alternating Kohn-Sham and DMFT impurity steps) are necessary for full convergence. Note that DFT+DMFT, contrary to conventional DFT, explicitly treats finite temperature. In all calculations presented in this scope, the temperature was set to $T = 145$ K. The large-scale calculations run in a parallelized computing architecture for the k -points of the DFT part as well as for the QMC sweeps. Computations also ask for a sizable memory due to the demanding supercell structures. Even on supercomputing machines, full convergence for an individual superlattice at a given finite temperature still asks for several days of computing time.

4 DFT+DMFT results for few-layer-doped SmTiO_3

Key interest is in both, the global behavior as well as the layer-resolved physics of these artificial $n\text{SrO}/\text{SmTiO}_3$ systems. Importantly, the given structurally well-defined doping of the Mott insulator, enables an account of the realistic many-body electron states which is free of the usual disorder effects in common bulk-doped materials.

We first focus on the global electronic system by inspecting the total spectral function, plotted in Fig. 2. In the effective single-particle picture of conventional DFT this function coincides with the density of states (DOS). The relevant DOS building blocks for the present transition-metal oxides are a dominantly O- $2p$ spectral part deep in the occupied region, a Ti- $3d(t_{2g})$ -like part at low energy and a Ti- $3d(e_g)$ -like part energetically higher in the unoccupied region. As a first observation, both theoretical schemes, DFT(GGA) and DFT+DMFT, mark the present COHs as metallic, in line with experiment^{8,9}. In addition,

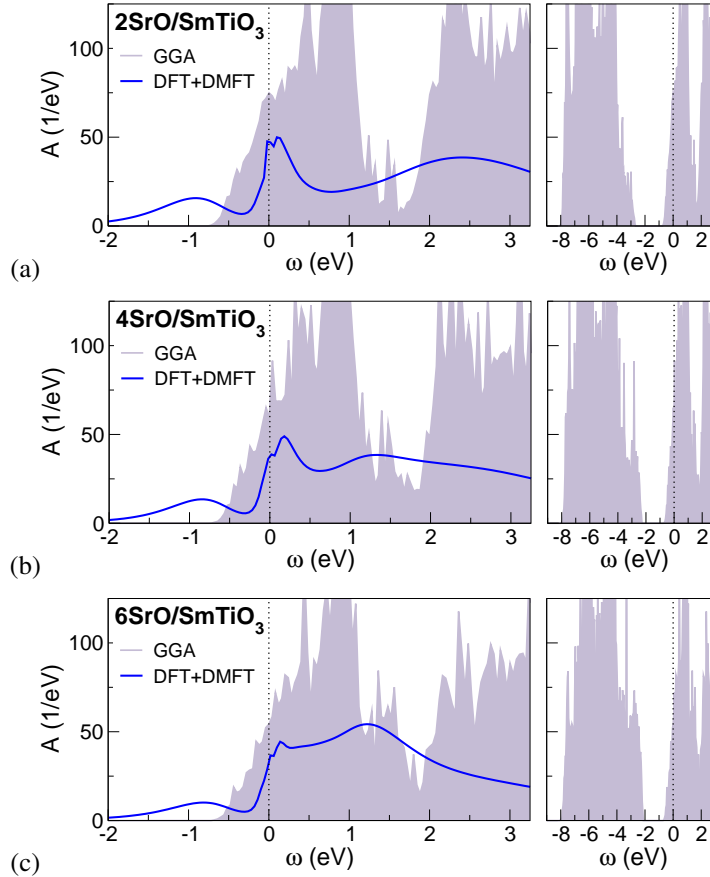


Figure 2. Total spectral function of SmTiO_3 doped with two (a), four (b) and six (c) layers of SrO compared to DFT(GGA). Right part shows the DFT density of states in a larger energy window, respectively, displaying the dominantly O- $(2p)$ block for energies $\sim [-8, -2]$ eV, the t_{2g} -like part around the Fermi level and the e_g -dominated states above 2 eV.

the $n = 1$ case of δ -doped SmTiO_3 is identified as conducting^{8,9,5}.

For a comparison of the different n SrO-doping cases it is important to realize that replacing $n > 1$ SmO layers with SrO ones actually results in new finite building blocks of effective SrTiO_3 . In bulk form, the latter perovskite is a band insulator with nominal $\text{Ti-}3d^0$ filling. Thus by increasing the number of SrO layers, the originally Mott-insulating system is replaced in parts by a band-insulating system. It is a particularly interesting scenario to have the different insulator concepts, i.e. the band insulator from band theory and the Mott insulator from interacting many-body theory, conjoint within a single electronic structure problem. Concretely, this means that the present doping with more and more SrO layers should not simply result in a successive strengthening of the metallic character. There are 28 Ti atoms in the supercell, which from $3d^1$ yields also 28 electrons in the occupied part of the spectral function. Each SrO layer, incorporating two Sr sites, adds two holes, resulting in a nominal doping of $1/14$ holes per Ti site. Accordingly, from $n = 2$ to $n = 6$ the Ti-dominated occupied part of the spectrum shrinks from 28 to 16 electrons, as visualized in Fig. 2. The degree of metallicity is more elusive since to a first approximation encoded in the height and width of the quasiparticle (QP) peak around the Fermi level. For $n = 2$, the QP peak is higher than for $n = 4$, but the width is slightly larger for the latter case. Compared to these cases, the QP peak is clearly diminished for $n = 6$. At higher energies in the occupied spectrum, DFT+DMFT accounts for the lower Hubbard band at ~ -0.9 eV, denoting the degree of real-space localization, which is missing in the DFT description. The transfer of spectral weight from the QP peak to the Hubbard peaks with increasing correlation strength is a hallmark of strongly correlated systems.

The competition between band-insulating and Mott-insulating tendencies becomes more obvious on the layer- and orbital-resolved local level. In the orthorhombic distorted systems, the $\text{Ti}(t_{2g})$ orbitals $|xz\rangle$, $|yz\rangle$ and $|xy\rangle$ hybridize on each site, forming effective crystal-field orbitals $|1\rangle$, $|2\rangle$ and $|3\rangle$ ^{17,4,5}. Though the linear combinations are layer-dependent, the qualitative character remains stable throughout the TiO_2 layers. In bulk SmTiO_3 , the d^1 electron majorly resides in the $|2\rangle$ orbital. Table 1 provides the multi-orbital fillings for the symmetry-inequivalent Ti1-8 sites in n -layer SrO/ SmTiO_3 . Figure 3 shows furthermore the local spectral functions for each choice of n for the given Ti sites, i.e. from the doping layers towards the bulk-like region of SmTiO_3 . Interestingly, when

SrO layers n	orbital	Ti1	Ti2	Ti3	Ti4	Ti5	Ti6	Ti7	Ti8
2	$ 1\rangle$	0.11	0.13	0.24	0.39	0.07	0.05	0.21	0.04
	$ 2\rangle$	0.13	0.13	0.53	0.46	0.89	0.93	0.71	0.96
	$ 3\rangle$	0.04	0.26	0.14	0.13	0.02	0.02	0.04	0.01
4	$ 1\rangle$	0.05	0.05	0.09	0.34	0.24	0.04	0.18	0.03
	$ 2\rangle$	0.04	0.04	0.08	0.35	0.63	0.93	0.81	0.96
	$ 3\rangle$	0.02	0.05	0.31	0.18	0.08	0.01	0.02	0.01
6	$ 1\rangle$	0.03	0.03	0.06	0.09	0.39	0.06	0.16	0.03
	$ 2\rangle$	0.02	0.02	0.05	0.09	0.32	0.90	0.82	0.97
	$ 3\rangle$	0.03	0.02	0.06	0.21	0.13	0.02	0.01	0.01

Table 1. $\text{Ti}(t_{2g})$ occupations from DFT+DMFT in the crystal-field basis within each TiO_2 layer of n -layer-doped SmTiO_3 .

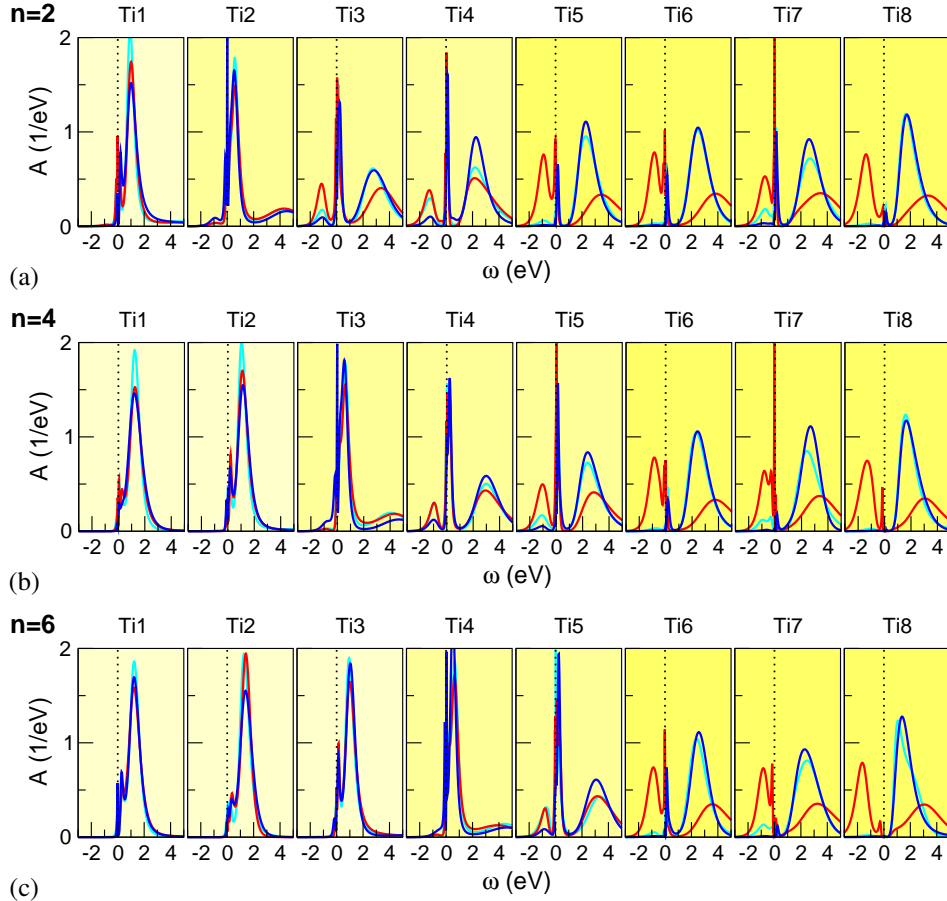


Figure 3. Local Ti- and orbital-resolved DFT+DMFT spectral function of SmTiO_3 doped with two (a), four (b) and six (c) layers of SrO. Colored curves denote the orbital flavor: |1>: lightblue, |2>: red and |3>: blue. Different colored backgrounds mark tendencies towards band-insulating (bright), metallic (light yellow) and Mott-critical (yellow) character.

embedded by the SrO layers, the system quickly establishes band-insulating-like behavior. Meaning, the Ti states become completely depleted and the region gets inaccessible for electron transport. On the other hand, far away from the SrO layers the system is Mott critical, i.e. either is in a doped-Mott or Mott-insulating regime. Inbetween these different insulating(-like) parts, a seemingly moderately-correlated metallic region of 2-3 TiO_2 -layers width is established, respectively. This metallic region shifts correspondingly with increasing n in the superlattices. Surprisingly for each n , in a single TiO_2 layer of these metallic parts there is orbital polarization towards state |3>, which is of dominant $|xy\rangle$, i.e. inplane, contribution. Thereby associated is high QP peak of identical orbital flavor. Since the system is strongly |2>-polarized in the Mott-critical region similar to the bulk compound, this additional polarization is a unique heterostructure effect. Note that it is absent for the δ -doped case $n = 1^5$, and hence could be important for the stronger

Fermi-liquid character in the cases $n > 1$ ⁸.

4.1 Summary

Large-scale first-principles many-body calculations based on the advanced DFT+DMFT framework are capable of addressing the challenging emerging physics of correlated oxide heterostructure on a realistic level. For the case of few-layer doped SmTiO₃, the coexistence of different electronic phases, i.e. band-insulating, metallic and Mott-critical are predicted on a multi-orbital level. In addition, alternating orbital polarizations are revealed, that open further engineering possibilities. In general, the richness of various competing real-space regions of different electronic kind in a single equilibrium system should enable various technological applications.

Acknowledgments

The author gratefully acknowledges the computing time granted by the John von Neumann Institute for Computing (NIC) and provided on the supercomputer JURECA at the Jülich Supercomputing Centre (JSC) under project number hhh08.

References

1. H. Y. Hwang, Y. Iwasa, M. Kawasaki, B. Keimer, N. Nagaosa, and Y. Tokura, *Emergent phenomena at oxide interfaces*, Nature Materials, **11**, 103, 2012.
2. J. Chakhalian, J. W. Freeland, A. J. Millis, C. Panagopoulos, and J. M. Rondinelli, *Emergent properties in plane view: Strong correlations at oxide interfaces*, Rev. Mod. Phys., **86**, 1189, 2014.
3. O. Janson, Z. Zhong, G. Sangiovanni, and K. Held, in *Spectroscopy of TMO interfaces*, chapter Dynamical mean field theory for oxide heterostructures, Springer, 2016.
4. F. Lechermann and M. Obermeyer, *Towards Mott design by δ -doping of strongly correlated titanates*, New J. Phys., **17**, 043026, 2015.
5. F. Lechermann, *Unconventional electron states in δ -doped SmTiO₃*, Sci. Rep, **7**, 1565, 2017.
6. G. Kotliar, S. Y. Savrasov, K. Haule, V. S. Oudovenko, O. Parcollet, and C. A. Marianetti, *Electronic structure calculations with dynamical mean-field theory*, Rev. Mod. Phys., **78**, 865, 2006.
7. A. C. Komarek, H. Roth, M. Cwik, W.-D. Stein, J. Baier, M. Kriener, F. Bourée, T. Lorenz, and M. Braden, *Magnetoelastic coupling in RTiO₃ (R=La,Nd,Sm,Gd,Y) investigated with diffraction techniques and thermal expansion measurements*, Phys. Rev. B, **75**, 224402, 2007.
8. C. A. Jackson, J. Y. Zhang, C. R. Freeze, and S. Stemmer, *Quantum critical behaviour in confined SrTiO₃ quantum wells embedded in antiferromagnetic SmTiO₃*, Nat. Commun., **5**, 4258, 2014.
9. E. Mikheev, C. R. Freeze, B. J. Isaac, T. A. Cain, and S. Stemmer, *Separation of transport lifetimes in SrTiO₃-based two-dimensional electron liquids*, Phys. Rev. B, **91**, 165125, 2015.

10. S. Y. Savrasov, G. Kotliar, and E. Abrahams, *Correlated electrons in δ -plutonium within a dynamical mean-field picture*, Nature, **410**, 793, 2001.
11. L. V. Pourovskii, B. Amadon, S. Biermann, and A. Georges, *Self-consistency over the charge density in dynamical mean-field theory: A linear muffin-tin implementation and some physical implications*, Phys. Rev. B, **76**, 235101, 2007.
12. D. Grieger, C. Piefke, O. E. Peil, and F. Lechermann, *Approaching finite-temperature phase diagrams of strongly correlated materials: A case study for V_2O_3* , Phys. Rev. B, **86**, 155121, 2012.
13. B. Meyer, C. Elsässer, F. Lechermann, and M. Fähnle, “Fortran 90 program for mixed-basis-pseudopotential calculations for crystals”.
14. J. P. Perdew, K. Burke, and M. Ernzerhof, *Generalized gradient approximation made simple*, Phys. Rev. Lett., **77**, 3865, 1996.
15. B. Amadon, F. Lechermann, A. Georges, F. Jollet, T. O. Wehling, and A. I. Lichtenstein, *Plane-wave based electronic structure calculations for correlated materials using dynamical mean-field theory and projected local orbitals*, Phys. Rev. B, **77**, 205112, 2008.
16. V. I. Anisimov, D. E. Kondakov, A. V. Kozhevnikov, I. A. Nekrasov, Z. V. Pchelkina, J. W. Allen, S.-K. Mo, H.-D. Kim, P. Metcalf, S. Suga, A. Sekiyama, G. Keller, I. Leonov, X. Ren, and D. Vollhardt, *Full orbital calculation scheme for materials with strongly correlated electrons*, Phys. Rev. B, **71**, 125119, 2005.
17. E. Pavarini, A. Yamasaki, J. Nuss, and O. K. Andersen, *How chemistry controls electron localization in $3d^1$ perovskites: a Wannier-function study*, New J. Phys., **7**, 188, 2005.
18. A. N. Rubtsov, V. V. Savkin, and A. I. Lichtenstein, *Continuous-time quantum Monte Carlo method for fermions*, Phys. Rev. B, **72**, 035122, 2005.
19. P. Werner, A. Comanac, L. de’ Medici, M. Troyer, and A. J. Millis, *Continuous-time solver for quantum impurity models*, Phys. Rev. Lett., **97**, 076405, 2006.
20. O. Parcollet, M. Ferrero, T. Ayril, H. Hafermann, I. Krivenko, L. Messio, and P. Seth, *TRIQS: A toolbox for research on interacting quantum systems*, Comput. Phys. Commun., **196**, 398, 2015.
21. P. Seth, I. Krivenko, M. Ferrero, and O. Parcollet, *TRIQS/CTHYB: A continuous-time quantum Monte Carlo hybridisation expansion solver for quantum impurity problems*, Comput. Phys. Commun., **200**, 274, 2016.
22. V. I. Anisimov, I. V. Solovyev, M. A. Korotin, M. T. Czyżyk, and G. A. Sawatzky, *Density-functional theory and NiO photoemission spectra*, Phys. Rev. B, **48**, 16929, 1993.